PHYSICAL REVIEW B **89**, 161101(R) (2014)

Galvanomagnetic and thermogalvanomagnetic transport effects in ferromagnetic fcc Co_xPd_{1-x} alloys from first principles

S. Wimmer,* D. Ködderitzsch, and H. Ebert

Department Chemie/Phys. Chemie, Ludwig-Maximilians-Universität München, Butenandtstrasse 11, 81377 München, Germany

(Received 11 November 2013; revised manuscript received 6 March 2014; published 2 April 2014)

The galvanomagnetic and thermogalvanomagnetic transport of the prototypical ferromagnetic transition-metal alloy system fcc Co_xPd_{1-x} has been investigated on the basis of Kubo's linear response formalism. The results for the full electric conductivity tensor allow discussing the spin-orbit-induced anisotropic magnetoresistance and the anomalous Hall effect. These are complemented by results for the corresponding thermogalvanomagnetic transport properties anisotropy of the Seebeck effect and anomalous Nernst effect. The relation between the respective response coefficients is discussed with the underlying electronic structure calculated relativistically within the Korringa-Kohn-Rostoker coherent potential approximation band structure method for disordered alloys.

DOI: 10.1103/PhysRevB.89.161101 PACS number(s): 71.15.Rf, 71.70.Ej, 72.15.Jf, 72.15.Qm

A ferromagnet subject to an external electric field and/or thermal gradient shows a plethora of interesting transport effects, with some of them already being exploited in technological applications. Depending on the direction of the magnetization such materials show a variation of the electric resistivity, denoted as anisotropic magnetoresistance (AMR). Furthermore the anomalous Hall effect (AHE) gives rise to components of the electric current transverse to the applied electric field. Both effects, present also in the absence of an external magnetic field, result from the relativistic coupling of spin and orbital degrees of freedom [spin-orbit coupling (SOC)].

The thermal counterparts to the AMR, the anisotropy of the Seebeck effect (ASE) and to the AHE, the anomalous Nernst effect (ANE) share the same origins. These anisotropic and anomalous effects pose challenges to a theoretical description starting from first principles, which is needed in order to give *material-specific* parameters. While the AMR and the closely related planar Hall effect have been extensively studied, there are relatively few experimental investigations on the ASE and planar Nernst effect (PNE) to be found in the literature [1–4], and, to our knowledge, so far only one first-principles study is available [5], which deals with the magnetic anisotropy of the transmission through a Cu|Co|Cu trilayer system and its enhancement due to the symmetry breaking at the Co|Cu interface. To a much greater extent investigations have been carried out on a closely related class of phenomena, namely the magneto-thermopower or -Seebeck effect and its variations (spin-dependent, tunneling, tunneling anisotropic) occurring in various types of heterostructures [6–9].

Concerning the AHE [10–13] and ANE [13,14], strong interest has arisen in recent years driven by progress in the understanding of the microscopic origins of transverse transport effects and by the (re)discovery of the spin Hall effect [15–17]. The latter also has its thermoelectric analog, the spin Nernst effect [18–20]. Disentangling the various contributions to the anomalous and spin Hall effects [21] has recently been supported by material-specific first-principles calculations. Apart from an intrinsic contribution, a pure band structure effect related to the Berry phase [14,22], there are extrinsic contributions due to scattering at impurities [11,12]. Usually those are related to skew or Mott scattering [23] and the side-jump mechanism [24] and are mainly discussed in the dilute limit. In recent years several first-principles calculations have been reported, dealing with the intrinsic parts of anomalous Hall conductivity (AHC) [25,26] and spin Hall conductivity (SHC) [27,28], a scattering-independent side-jump contribution to the AHE [26,29] and the skew scattering in the SHE [30,31]. To a lesser extent studies exist treating *all* contributions on equal footing on a first-principles level [31–34].

The thermally induced electron (and spin) transport, which is much less explored on a quantitative theoretical level than the responses to an electric field, has recently gained tremendous impetus giving rise to the new field of spin caloritronics [35]. Since there already exists a great deal of insight into the microscopic mechanisms responsible for longitudinal and transverse galvanomagnetic transport effects, and their thermal counterparts share the same origin—namely the spin-orbit interaction—one has an obvious starting point for detailed investigations of the latter. Concerning explicitly spin-dependent effects first-principles work has been done for the spin Nernst effect using the Boltzmann formalism [36] and Kubo linear response theory [37]. So far no clear-cut experimental verification of this phenomenon could be made, but there is substantial evidence [38]. For the symmetric part of the corresponding response tensor (see below) Slachter *et al*. [39] were able to show that indeed a spin-dependent Seebeck effect exists and later on the same group reported the observation of its reciprocal, the spin-dependent Peltier effect [40]. The interest in the implicitly spin-dependent phenomena (ASE/PNE [2–4] and ANE [3,41–43]) has been revived lately by the fact that in experiments on the recently discovered spin Seebeck effect (SSE) [44] its signal has to be disentangled from those of the aforementioned effects having the same symmetry [4,41,43,45].

It is therefore crucial to have a quantitative description of those effects at hand in order to be able to extract the true spin Seebeck signal. So far only a very few such investigations

*sebastian.wimmer@cup.uni-muenchen.de

have been carried out, e.g., for the ANE [14,46], but to our knowledge not for the ASE/PNE and in particular not for disordered alloys. This Rapid Communication aims at filling this gap by presenting results for various galvanomagnetic and thermogalvanomagnetic properties (AMR, ASE, AHE, and ANE) of a prototypical ferromagnetic alloy, namely $Co_{1-x}Pd_x$. Using the concentration as an independent parameter allows varying electronic properties and the strength of the spin-orbit interaction.

Kubo's linear response formalism allows relating the electric current densities $\vec{j}^{\,c}$ to the gradients of the electrochemical potential μ and temperature T [47,48]:

$$\vec{j}^{\,c} = -L^{cc}\vec{\nabla}\mu - L^{cq}\vec{\nabla}T/T, \tag{1}$$

with the gradient of the electrochemical potential $\vec{\nabla}\mu = \vec{\nabla}\mu_c + e\vec{E}$, where μ_c is the chemical potential, $e = |e|$ the elementary charge and $\vec{E}$ the electric field. Furthermore $\vec{\nabla}T$ denotes the temperature gradient. All elements of the second rank response tensors L^{ij} will be considered as temperature dependent with the restriction to the electronic temperature T, i.e., the phononic and magnonic temperatures are neglected. The response tensors appearing in Eq. (1) can be calculated from the corresponding conductivities in the athermal limit (see Smrčka and Středa [49] or Jonson and Mahan [50]). For the electric field along ν, with $\mu,\nu \in \{x,y,z\}$ one has:

$$L^{cc}_{\mu\nu}(T) = -\frac{1}{e}\int dE\, \sigma^{cc}_{\mu\nu}(E) D(E,T), \tag{2}$$

with $D(E,T) = (-\frac{\partial f(E,T)}{\partial E})$, $f(E,T)$ the Fermi function, and the energy-dependent charge conductivity $\sigma^{cc}_{\mu\nu}(E)$, which is obtained by applying the Kubo-Středa formalism. In the zero temperature limit one has $-eL^{cc} \equiv \sigma^{cc}(E_F)$, with E_F being the Fermi energy.

Assuming Cartesian coordinates and the sample being a cubic collinear magnet with magnetization pointing in the z direction the conductivity tensor has the structure (all the following quantities are given for that particular symmetry of the system) [51]:

$$\sigma^{cc} = \begin{pmatrix} \sigma_{xx} & \sigma_{xy} & 0 \\ -\sigma_{xy} & \sigma_{xx} & 0 \\ 0 & 0 & \sigma_{zz} \end{pmatrix}. \tag{3}$$

The tensor for the residual resistivity is obtained by inversion of the conductivity tensor: $\rho = (\sigma^{cc})^{-1}$ and with the assumed symmetry restriction the isotropic resistivity is $\rho_{iso} = \mathrm{Tr}(\rho) = (2\rho_{xx} + \rho_{zz})/3$.

The anisotropic magnetoresistance (AMR), describing the resistance of the magnetic system dependent on the mutual angle of magnetization and current driving electric field is given by

$$\Delta\rho = \rho_{zz} - \rho_{xx} \tag{4}$$

and the so called AMR ratio by $\Delta\rho/\rho_{iso}$. Finally, the anomalous Hall conductivity is given by the off-diagonal element σ_{xy} in Eq. (3).

The transport coefficient $L^{cq}_{\mu\nu}(T)$ is expressed through the energy dependence of the electric conductivity $\sigma^{cc}_{\mu\nu}(E)$ as [49,50]:

$$L^{cq}_{\mu\nu}(T) = -\frac{1}{e}\int dE\, \sigma^{cc}_{\mu\nu}(E)\, D(E,T)\,(E - E_F). \tag{5}$$

Considering a thermal gradient $\vec{\nabla}T$ without an external electric field $\vec{E}$ the resulting electric current $\vec{j}^{\,c}$ vanishes when open-circuit conditions are imposed. Equation (1) implies that an internal electric field

$$\vec{E} = -\frac{1}{eT}(L^{cc})^{-1}L^{cq}\vec{\nabla}T = S\,\vec{\nabla}T \tag{6}$$

builds up in order to compensate the charge imbalance induced by $\vec{\nabla}T$, where S is the thermogalvanomagnetic tensor. It has been shown by various authors (cf., e.g., Ref. [50]) that the expression for S implied by Eq. (6) reduces to the original expression of Mott for $T \to 0$ K. Obviously, the resulting Seebeck effect connected with longitudinal transport is expressed by the diagonal elements of the tensor

$$S = \sigma^{-1}\alpha\ . \tag{7}$$

On the other hand the pure ANE—which is not restricted to the open-circuit condition—connected with transverse transport is represented in the following by the off-diagonal elements of the tensor α^{cq} (or L^{cq}). The chosen notation is in line with the conventional symbol $\alpha^{cq}_{\mu\nu} = -L^{cq}_{\mu\nu}/T$ for the Nernst [41,42,46] (or Peltier [52]) coefficient or conductivity.

To investigate the transport properties of the ferromagnetic fcc Co_xPd_{1-x}, seen as a prototype transition-metal alloy system, in a most detailed way its electronic structure has been determined in a first step by means of the fully relativistic version of the Korringa-Kohn-Rostoker (KKR) band structure method [53]. The corresponding calculations have been done self-consistently within the framework of local spin density functional theory (LSDA) with the substitutional disorder in the alloys accounted for by the coherent potential approximation (CPA). In a second step, the transport coefficients L^{cc} and L^{cq} were determined using Eqs. (2) and (5), respectively, on the basis of the Kubo-Středa formalism [31,32,54,55]. For the athermal limit Mott's classical formula for the thermopower to obtain S/T and α/T has been used. It should be noted that, whereas for determining the symmetric part of the conductivity tensor [see Eq. (3)] the Kubo-Greenwood approach is sufficient, for the calculation of the antisymmetric components a Kubo-Středa or Kubo-Bastin approach is needed.

Figure 1 shows the residual resistivity ρ_{iso} of Co_xPd_{1-x} as a function of the composition in comparison with experiment. As one notes, ρ_{iso} has a maximum at around 20% Co, which is more pronounced for the calculations as in experiment [56], for which it is probably not fully resolved. The strong deviation from the Nordheim rule, which implies a symmetric and parabolic dependence of ρ_{iso} on the concentration x, can be explained by details of the electronic structure (see below). A well-known property of the Co_xPd_{1-x} system is its rather high anisotropic magnetoresistance (AMR), which is one of the largest found in binary transition-metal alloys,

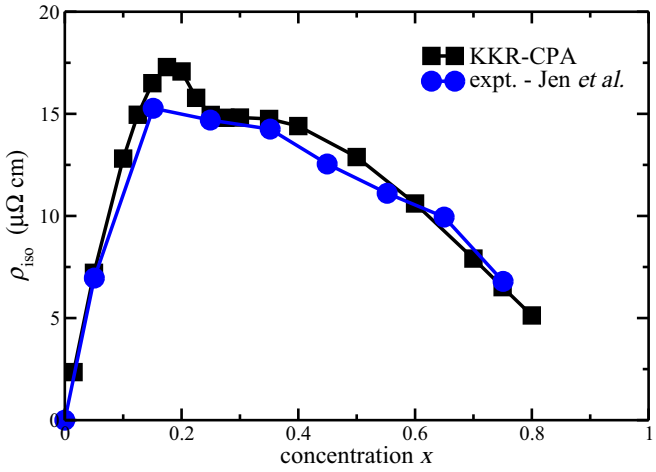

FIG. 1. (Color online) Calculated (squares) and experimental [56] (circles) isotropic residual resistivity ρ_{iso} of Co_xPd_{1-x} as a function of alloy composition.

although not as large as in Fe_xNi_{1-x} or Co_xNi_{1-x} alloys. The calculated AMR ratio is shown in Fig. 2 (top) together with experimental results [57]. Its steep rise between 0 and approximately 20–25 % Co is consistent with experiment. For higher Co concentrations the experimental value stays nearly constant over a large concentration range (approximately up to 70% Co), while the theoretical value drops. A possible reason for this discrepancy could be structural inhomogeneities of the investigated samples, e.g., caused by clustering.

The Seebeck coefficients S_{ii} for transport perpendicular (xx) and parallel (zz) to the magnetization are shown in terms of $-S_{ii}/T$ in Fig. 2 (bottom). As one notes these quantities show a very prominent maximum slightly above 20% Co and differ in particular in the region of the maximum. The corresponding anisotropy of the Seebeck effect (ASE) can be expressed in terms of the ratio:

$$\mathrm{ASE} = \frac{S_{xx} - S_{zz}}{\frac{2}{3}S_{xx} + \frac{1}{3}S_{zz}} = \frac{\Delta S_{ii}}{S_{\mathrm{iso}}}. \tag{8}$$

As one can see in Fig. 2 (bottom) the ASE ratio also shows a maximum at 20% Co, slightly lower than the AMR in the top figure, reaching nearly the value of 0.2. In contrast to the Seebeck coefficient itself, the ASE ratio still shows appreciable values away from the maximum region as well. Here one should note that so far relatively few experimental investigations on the ASE (or PNE) can be found in the literature [1,2,4,43]. Measurements on the diluted ferromagnetic semiconductor $Ga_{1-x}Mn_xAs$, for example, gave for $x = 0.039$ a value of around 6% at 6 K [2], which is clearly lower than the maximum value for Co_xPd_{1-x} found here.

The use of Mott's formula for the Seebeck coefficient implies an extrapolation $T \to 0$ K (athermal limit) leading to a constant value for $-S_{ii}/T$. Using instead the generalized Mott formula as given by Eq. (5) $S_{ii}(T)$ has to be calculated for each individual temperature T. Figure 3 shows for $Co_{0.2}Pd_{0.8}$ the Seebeck coefficients S_{xx} and S_{zz} as a function of the temperature. As one notes, there are clear deviations from the simple linear behavior expected from Mott's formula for higher temperatures. In addition, one finds that the individual temperature dependence of S_{xx} and S_{zz} leads to an appreciable temperature dependence of the ASE ratio with a broad

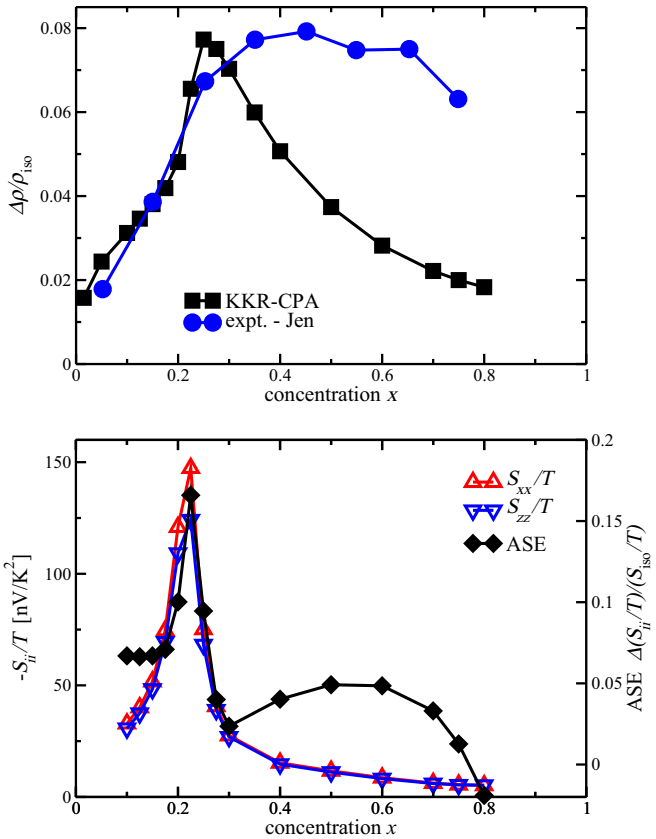

FIG. 2. (Color online) (Top) Calculated (squares) and experimental [57] (circles) AMR ratio $\Delta\rho/\rho_{iso}$ of Co_xPd_{1-x}. (Bottom) Calculated Seebeck coefficients in terms of $-S_{ii}/T$ for transport perpendicular (xx) and parallel (zz) to the magnetization for the athermal limit $T \to 0$ K. In addition the anisotropy of the Seebeck coefficient (ASE) calculated by Eq. (8) is given.

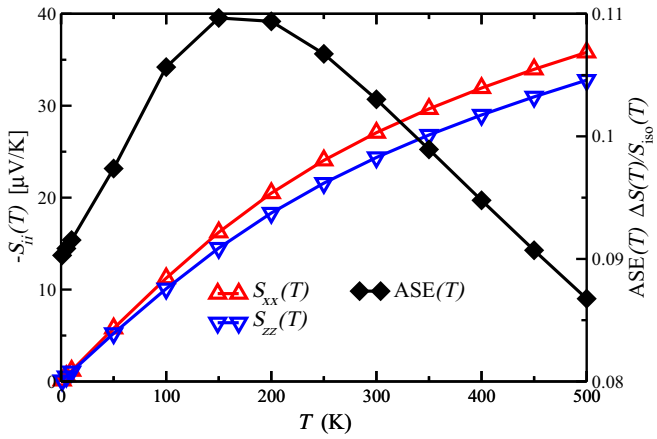

FIG. 3. (Color online) Temperature dependence of the calculated Seebeck coefficients S_{xx} and S_{zz} (triangles up and down, respectively) in $Co_{0.2}Pd_{0.8}$. In addition the corresponding anisotropy ratio ASE $= (S_{xx} - S_{zz})/(\frac{2}{3}S_{xx} + \frac{1}{3}S_{zz})$ is shown.

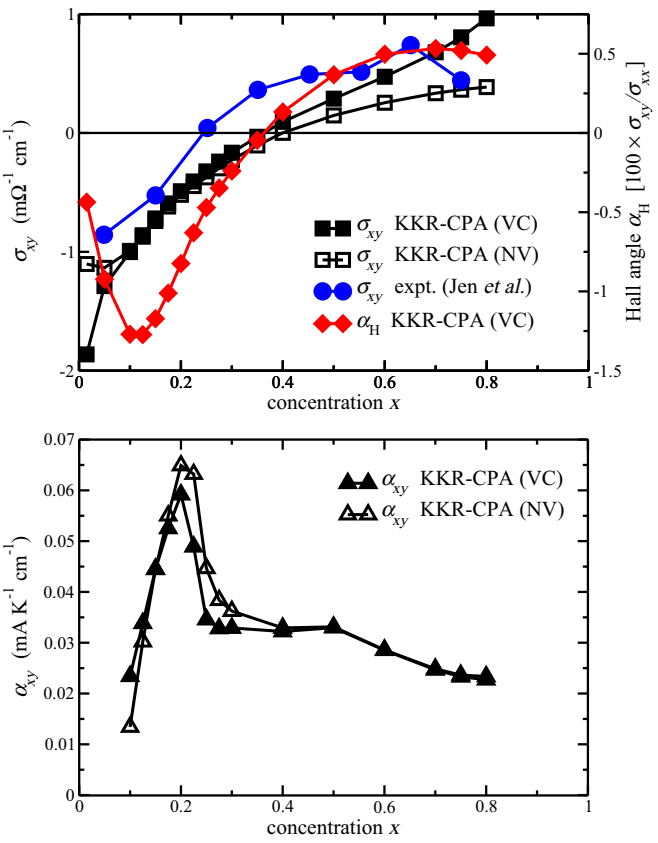

FIG. 4. (Color online) (Top) Calculated AHC (VC, full squares) together with its intrinsic contribution (NV, open squares) in comparison to low temperature experimental data [58] (circles). In addition the theoretical Hall angle $\alpha_H = \sigma_{xy}/\sigma_{xx}$ is shown. (Bottom) Calculated ANC α_{xy} (VC, full triangles) together with its intrinsic contribution (NV, open triangles), in the athermal limit.

maximum around 150 K. (One should bear in mind that the influence of phonons and magnons is not accounted for in these calculations, which might not be negligible in this system. In fact the Curie temperature for the alloy with 20% Co is around 500 K [60].)

The calculated AHC σ_{xy} of Co_xPd_{1-x} for $T = 0$ K shown in Fig. 4 (top) is found in very satisfying agreement with the corresponding low-temperature experimental data [58]. In addition to the theoretical AHC that includes the so-called vertex corrections (VC) [13,54], results are given for which these were ignored (NV). The difference between these can be identified with the extrinsic contributions to σ_{xy} due to the skew scattering and side-jump mechanisms [21,32]. Obviously, there are pronounced extrinsic contributions in the Pd-rich as well as Co-rich regimes having different sign. This situation is very similar to that found for the spin Hall effect in nonmagnetic transition-metal alloys [31]. In addition the figure shows the Hall angle $\alpha_H = \sigma_{xy}/\sigma_{xx}$ that—as the AHC σ_{xy}—shows a sign change at around 35% Co. This is followed by a very broad maximum around around 75% Co.

The anomalous Nernst conductivity (ANC) α_{xy} for $T \to 0$ corresponding to σ_{xy} is given in the bottom panel of Fig. 4. Again a very prominent maximum around 20% Co is found. As for the AHC, Fig. 4 (bottom) gives results for calculations including (VC) and excluding the vertex corrections. In contrast to σ_{xy}, these are relatively weak and remarkable only for the Pd-rich side of the system. Altogether the intrinsic contribution is dominant for all concentrations. As one notes from Fig. 4 there is no obvious direct relation between these transverse thermoelectric and electric transport coefficients α_{xy} and σ_{xy}, respectively (see below and Supplemental Material [59]).

The prominent maximum of the longitudinal transport quantities ρ_{iso} and $\Delta\rho/\rho_{iso}$ shown in Figs. 1 and 2, respectively, can be understood by having a look at the variation of the electronic structure of Co_xPd_{1-x} with its composition (see Supplemental Material [59]). For the majority channel, the upper edges of the d-like bands at the X and W points in the Brillouin zone touch the Fermi level for around 20% Co. The latter in fact extends over almost the whole length of the Z direction connecting W and X. For the minority spin channel, on the other hand, the Fermi level crosses sp-like bands that have a steep slope leading to a very different conductivity for the two spin channels. The peculiar features of the electronic structure of Co_xPd_{1-x} and its concentration dependence clearly also determine the behavior of the more complex transport quantities S_{ii} (and the associated ASE), σ_{xy} and α_{xy}. Concerning the transverse AHC σ_{xy} one has to account in addition for the prominent role of the spin-orbit coupling that has a rather different strength for the two alloy partners.

As mentioned above, there is no simple relationship between the galvanomagnetic and their corresponding thermogalvanomagnetic quantities, as AMR and ASE and AHC and ANC, respectively. This has to be ascribed to the fact that σ_{xy} is determined by the electronic structure in the range k_BT around the Fermi energy E_F, while for α_{xy} the first-order weight $(E - E_F)$ enters in addition the corresponding calculation.

In summary, a first-principles description of the galvanomagnetic and thermogalvanomagnetic properties of the prototypical ferromagnetic transition-metal alloy system Co_xPd_{1-x} has been presented. The results are in satisfying agreement with corresponding available experimental results. The prominent features of the concentration dependence of the various transport properties could be related to characteristic features of the underlying electronic structure as well as to the prominent role of spin-orbit coupling. In particular for a concentration of 20% Co in Pd a rather high ASE of around 10% was found, exhibiting an interesting nonlinear temperature dependence. For longitudinal as well as transverse responses to electric field and temperature gradient, different concentration dependences were found, which clearly shows that there is no trivial relation between the two classes of phenomena. The pronounced sensitivity of the galvanomagnetic and, to an apparently even greater extent, thermogalvanomagnetic transport effects to the electronic structure obviously allows tuning them in a relatively wide range by varying the composition of a substitutional alloy system.

This work was supported financially by the Deutsche Forschungsgemeinschaft (DFG) via the priority programme SPP 1538 and the SFB 689.

[1] V. D. Ky, Phys. Stat. Sol. (b) **17**, K207 (1966).
[2] Y. Pu, E. Johnston-Halperin, D. D. Awschalom, and J. Shi, Phys. Rev. Lett. **97**, 036601 (2006).
[3] A. Slachter, F. L. Bakker, and B. J. van Wees, Phys. Rev. B **84**, 020412 (2011).
[4] A. D. Avery, M. R. Pufall, and B. L. Zink, Phys. Rev. B **86**, 184408 (2012).
[5] V. Popescu and P. Kratzer, Phys. Rev. B **88**, 104425 (2013).
[6] L. Gravier, S. Serrano-Guisan, F. Reuse, and J.-P. Ansermet, Phys. Rev. B **73**, 024419 (2006).
[7] M. Czerner, M. Bachmann, and C. Heiliger, Phys. Rev. B **83**, 132405 (2011).
[8] M. Walter *et al*., Nature Mater. **10**, 742 (2011).
[9] Ts. Naydenova, P. Dürrenfeld, K. Tavakoli, N. Pégard, L. Ebel, K. Pappert, K. Brunner, C. Gould, and L. W. Molenkamp, Phys. Rev. Lett. **107**, 197201 (2011).
[10] R. Karplus and J. M. Luttinger, Phys. Rev. **95**, 1154 (1954).
[11] A. Crépieux and P. Bruno, Phys. Rev. B **64**, 014416 (2001).
[12] S. Onoda, N. Sugimoto, and N. Nagaosa, Phys. Rev. B **77**, 165103 (2008).
[13] N. A. Sinitsyn, J. Phys.: Cond. Mat. **20**, 023201 (2008).
[14] D. Xiao, Y. Yao, Z. Fang, and Q. Niu, Phys. Rev. Lett. **97**, 026603 (2006).
[15] M. Dyakonov and V. Perel, Phys. Lett. A **35**, 459 (1971).
[16] J. E. Hirsch, Phys. Rev. Lett. **83**, 1834 (1999).
[17] J. Sinova, D. Culcer, Q. Niu, N. A. Sinitsyn, T. Jungwirth, and A. H. MacDonald, Phys. Rev. Lett. **92**, 126603 (2004).
[18] S. G. Cheng, Y. Xing, Q. F. Sun, and X. C. Xie, Phys. Rev. B **78**, 045302 (2008).
[19] X. Liu and X. Xie, Solid State Commun. **150**, 471 (2010).
[20] Z. Ma, Solid State Commun. **150**, 510 (2010).
[21] N. Nagaosa, J. Sinova, S. Onoda, A. H. MacDonald, and N. P. Ong, Rev. Mod. Phys. **82**, 1539 (2010).
[22] M. Gradhand *et al*., J. Phys.: Cond. Mat. **24**, 213202 (2012).
[23] J. Smit, Physica **21**, 877 (1955).
[24] L. Berger, Phys. Rev. B **2**, 4559 (1970).
[25] X. Wang, D. Vanderbilt, J. R. Yates, and I. Souza, Phys. Rev. B **76**, 195109 (2007).
[26] J. Weischenberg, F. Freimuth, J. Sinova, S. Blügel, and Y. Mokrousov, Phys. Rev. Lett. **107**, 106601 (2011).
[27] Y. Yao and Z. Fang, Phys. Rev. Lett. **95**, 156601 (2005).
[28] G. Y. Guo, S. Murakami, T.-W. Chen, and N. Nagaosa, Phys. Rev. Lett. **100**, 096401 (2008).
[29] A. A. Kovalev, J. Sinova, and Y. Tserkovnyak, Phys. Rev. Lett. **105**, 036601 (2010).
[30] M. Gradhand, D. V. Fedorov, P. Zahn, and I. Mertig, Phys. Rev. Lett. **104**, 186403 (2010).
[31] S. Lowitzer, M. Gradhand, D. Ködderitzsch, D. V. Fedorov, I. Mertig, and H. Ebert, Phys. Rev. Lett. **106**, 056601 (2011).
[32] S. Lowitzer, D. Ködderitzsch, and H. Ebert, Phys. Rev. Lett. **105**, 266604 (2010).
[33] I. Turek, J. Kudrnovský, and V. Drchal, Phys. Rev. B **86**, 014405 (2012).
[34] D. Ködderitzsch, K. Chadova, J. Minár, and H. Ebert, New J. Phys. **15**, 053009 (2013).
[35] G. E. Bauer, A. H. MacDonald, and S. Maekawa, Solid State Commun. **150**, 459 (2010).
[36] K. Tauber, M. Gradhand, D. V. Fedorov, and I. Mertig, Phys. Rev. Lett. **109**, 026601 (2012).
[37] S. Wimmer, D. Ködderitzsch, K. Chadova, and H. Ebert, Phys. Rev. B **88**, 201108(R) (2013).
[38] T. Seki, I. Sugai, Y. Hasegawa, S. Mitani, and K. Takanashi, Solid State Commun. **150**, 496 (2010).
[39] A. Slachter, F. L. Bakker, J.-P. Adam, and B. J. van Wees, Nature Phys. **6**, 879 (2010).
[40] J. Flipse, F. L. Bakker, A. Slachter, F. K. Dejene, and B. J. van Wees, Nature Nanotechnol. **7**, 166 (2012).
[41] Y. Pu, D. Chiba, F. Matsukura, H. Ohno, and J. Shi, Phys. Rev. Lett. **101**, 117208 (2008).
[42] S. Y. Huang, W. G. Wang, S. F. Lee, J. Kwo, and C. L. Chien, Phys. Rev. Lett. **107**, 216604 (2011).
[43] M. Schmid, S. Srichandan, D. Meier, T. Kuschel, J.-M. Schmalhorst, M. Vogel, G. Reiss, C. Strunk, and C. H. Back, Phys. Rev. Lett. **111**, 187201 (2013).
[44] K. Uchida *et al*., Nature (London) **455**, 778 (2008).
[45] M. Weiler *et al*., Phys. Rev. Lett. **108**, 106602 (2012).
[46] J. Weischenberg, F. Freimuth, S. Blügel, and Y. Mokrousov, Phys. Rev. B **87**, 060406 (2013).
[47] R. Kubo, J. Phys. Soc. Japan **12**, 570 (1957).
[48] J. M. Luttinger, Phys. Rev. **135**, A1505 (1964).
[49] L. Smrčka and P. Středa, J. Phys. C: Solid State Phys. **10**, 2153 (1977).
[50] M. Jonson and G. D. Mahan, Phys. Rev. B **21**, 4223 (1980).
[51] W. H. Kleiner, Phys. Rev. **142**, 318 (1966).
[52] H. Kontani, Phys. Rev. B **67**, 014408 (2003).
[53] H. Ebert, D. Ködderitzsch, and J. Minár, Rep. Prog. Phys. **74**, 096501 (2011).
[54] W. H. Butler, Phys. Rev. B **31**, 3260 (1985).
[55] J. Banhart, R. Bernstein, J. Voitländer, and P. Weinberger, Solid State Commun. **77**, 107 (1991).
[56] S. U. Jen, T. P. Chen, and S. A. Chang, J. Appl. Physics **70**, 5831 (1991).
[57] S. U. Jen, Phys. Rev. B **45**, 9819 (1992).
[58] S. U. Jen, B. L. Chao, and C. C. Liu, J. Appl. Physics **76**, 5782 (1994).
[59] See Supplemental Material at http://link.aps.org/supplemental/10.1103/PhysRevB.89.161101 for a discussion of the changes in the electronic structure of Co_xPd_{1-x} alloys around $x \approx 0.2$ and their implications for transport properties. Furthermore the connection between galvanomagnetic and thermogalvanomagnetic effetcs is illustrated by means of the energy dependence of the anomalous Hall conductivity and the temperature dependence of the anomalous Nernst conductivity.
[60] R. M. Bozorth, P. A. Wolff, D. D. Davis, V. B. Compton, and J. H. Wernick, Phys. Rev. **122**, 1157 (1961).